



# Numerical Study of Cavitation in Francis Turbine of a Small Hydro Power Plant

P. P. Gohil<sup>†</sup> and R. P. Saini

*Alternate Hydro Energy Centre, Indian Institute of Technology Roorkee 247667, India*

<sup>†</sup>*Corresponding Author Email: p\_gohil@rediffmail.com*

(Received September 24, 2014; accepted January 30 2015)

## ABSTRACT

Cavitation is undesirable phenomena and more prone in reaction turbines. It is one of the challenges in any hydro power plant which cause vibration, degradation of performance and the damage to the hydraulic turbine components. Under the present study, an attempt has been made to carry out a numerical analysis to investigate the cavitation effect in a Francis turbine. Three dimensional numerical study approach of unsteady and SST turbulence model are considered for the numerical analysis under multiphase flow such as cavitating flow. The performance parameters and cavitating flow under different operating conditions have been predicted using commercial CFX code. Three different operating conditions under cavitation and without cavitation with part load and overload conditions of the turbine for a plant sigma factor are investigated. The results are presented in the form of efficiency, pressure fluctuation, vortex rope and vapor volume fraction.

It has been observed that variation in efficiency and vapor volume fraction is found to be nominal between cavitation and without cavitation conditions at rated discharge and rated head. Turbine efficiency loss and vapor bubbles formation towards suction side of the runner blade are found to be maximum under overload condition. However, the pressure pulsation has been found maximum under part load condition in the draft tube. The simulation results are found to be in good agreement with model test results for efficiency. The locations of cavitating zone observed well with the result of previous studies.

**Keywords:** Cavitation; Francis Turbine; Efficiency; CFX

## 1. INTRODUCTION

Basically small hydro power plant has less environment and social impacts compare to large hydro. The hydro power plant up to 25 MW is classified as small hydro in India and lot of potential is available to tap it in cost effective manner. In any hydro power plant, turbine is considered the main component which converts potential energy of water into electrical energy through electrical generator. Impulse and reaction types of hydro turbines are classified based on the water action on the runner. The reaction turbine is most suitable for medium head however it is more prone to cavitation effect.

Based on the literature review, Francis turbine has the highest percentile distribution of application in all continents (Water Power and Dam Construction Yearbook, 2006;2009). Technology is quite well developed and claimed mechanical efficiency over 95%. However, the turbine component shows the decline performance after few years of operation as they get damaged mainly due to cavitation, silt erosion, material defects and fatigue. Cavitation is

one of the undesirable phenomena in any hydro power plant. Cavitation may occur when the local static pressure in a fluid reaches below vapor pressure of the liquid at local temperature. In high velocity region of a turbine, the pressure can go down to a very low value that causes formation of small vapor bubbles, which then collapse suddenly. This phenomenon is called cavitation which leads to erosion pitting on the surface. This results in increase in energy loss, production of noise, vibration and reduces life of the components. It is therefore, there is a need to predict the cavitation in hydro turbine. The tendency for a flow to cavitate is characterized by the cavitation number or Thoma's cavitation factor ( $\sigma$ ) is expressed as below:

$$\sigma = \frac{H_a - H_v - H_s}{H} \quad (1)$$

where;  $H_a$  is the atmospheric pressure head [m],  $H_v$  is the vapor pressure in corresponding to the water temperature [m],  $H_s$  is the suction pressure at the outlet of reaction turbine or height of the turbine runner above the tail water surface [m],  $H$  is the net head of the turbine [m]. A flow is

cavitates if the cavitation number ( $\sigma$ ) is lower than the critical cavitation value ( $\sigma_c$ ) or plant cavitation factor ( $\sigma_p$ ).

The challenge is to run hydro turbines at maximum efficiency under different operating conditions for any hydro power plants. The traditional process of design is based on experiments, measurements and model testing which implies lots of money and time investment. The numerical simulation of the flow or Computational Fluid Dynamics (CFD) has been adopted as a tool for predicting performance parameters and fluid dynamics characteristics. CFD provides a cost effective and accurate alternative to scale model testing with variations on the simulation being performed quickly. In advancement of CFD, CFX code has used Rayleigh-Plesset (R-P) equation for cavitation analysis. It is widely used for the numerical modeling of complex real cavitating flows by assuming that the liquid carries cavitation nuclei whose growth is controlled by the R-P equation. This is a simple way to account the production of vapor in a cavitating flow by pressure reduction. The corresponding source term is introduced in the continuity equation for the vapor phase which is solved numerically together with the Navier-Stokes equation for the liquid/vapor mixture. This approach makes it possible to develop guidelines for the analysis of the influence of flow velocity on the erosive potential of a cavitating flow (Franck, 2007).

A number of numerical and experimental based researches on cavitation in different hydro turbo machines have been carried out and are available in literature. The different aspects of complex cavitation phenomenon have been discussed viz; bubble collapse, erosion damage, cavitation acoustics, cloud cavitation and rotating cavitation (Wang G. *et al.*, 2001; Wang Y.C. *et al.*, 1994; Avellan *et al.*, 1990; Avellan *et al.*, 2003). The 3D cavitating flow in the GAMM Francis runner has been carried out at best efficiency point and the cavity shape and position were investigated having a good agreement with the flow visualization (Bernad *et al.*, 2004). The cavitation model using R-P equation was developed and validated for the flow around a hemispherical fore-body and NACA 009 hydrofoil (Bernad *et al.*, 2004; Bernad *et al.*, 2006).

Under this study an attempt has been made to carry out investigations on unsteady cavitating flow analysis in Francis turbines at part load, rated load (BEP) and overload conditions. The simulation has been performed in operating range from part load (40% rated load) to over load (130% rated load) with transient condition and viscous flow turbulence Shear Stress Transport (SST) model using CFX code. In order to predict the performance and cavitating flow behavior of a prototype Francis turbine having a rated capacity of 200 kW has been considered for the present investigation. It is a medium specific speed turbine and the specifications of the turbine are given in Table 1.

**Table 1 Parameter of Francis turbine**

Sr. No.	Parameter	Value
1	Rated power [kW]	200
2	Rated flow rate [m <sup>3</sup> /s]	0.850
3	Rated head [m]	24.25
4	Rotational speed [rpm]	750
5	Number of runner blade [-]	15
6	Number of guide vane [-]	12
7	Number of stay vane [-]	12
8	Diameter of runner [mm]	465

## 2. MATHEMATICAL FORMULATION

### 2.1 Governing Equations:

The governing equations consist of the conservative from the Reynolds Averaged Navier-Stokes equation and a volume fraction transport equation. These equations used are the continuity equation and the momentum equation which can be expressed as;

$$\frac{\partial \rho_m}{\partial t} + \frac{\partial(\rho_m u_j)}{\partial x_j} = 0 \tag{2}$$

$$\frac{\partial(\rho_m u_i)}{\partial t} + \frac{\partial(\rho_m u_j u_i)}{\partial x_j} = -\frac{\partial p}{\partial x_i} + A + B \tag{3}$$

where,  $A = \frac{\partial}{\partial x_j} \left[ (\mu_m + \mu_t) \left( \frac{\partial u_i}{\partial x_j} + \frac{\partial u_j}{\partial x_i} \right) \right]$ ,

$$B = -\rho_m \omega u_i - \rho_m \omega (\omega \cdot r)$$

### 2.2 Transport Equation:

The liquid-vapor mass transfer due to cavitation governed by the vapor volume fraction transport is expressed by the following equation:

$$\frac{\partial(\rho_v \alpha)}{\partial t} + \frac{\partial(\rho_v \alpha u_j)}{\partial x_j} = S_\alpha = \dot{m}^v + \dot{m}^c \tag{4}$$

where,  $\rho_v$  is the vapor density;  $\alpha_v$  is the vapor volume fraction;  $\dot{m}^v$  and  $\dot{m}^c$  are the mass transfer rates correspond to the evaporation and condensation respectively during cavitation process

The mixture density  $\rho_m$  and the mixture dynamic viscosity  $\mu$  are defined as;

$$\rho_m = \rho_v \alpha_v + \rho_l (1 - \alpha_v) \tag{5}$$

$$\mu = \mu_v \alpha_v + \mu_l (1 - \alpha_v) \tag{6}$$

where,  $\rho_l$  is the liquid density, and  $\mu_v$  and  $\mu_l$  are the vapor viscosity and liquid viscosity, respectively.

### 2.3 Turbulence Model:

The equation used in the Shear Stress Transport model for the mixture can be expressed as;

$$\mu_T^m = \frac{\rho_m a_1 k^m}{\max(a_1 \omega^m, S^m F_2)} \tag{7}$$

where,  $k$  is the turbulent kinetic energy,  $\omega$  is the turbulent frequency,  $F_2$  is the blending function,  $\mu_T$  is the turbulent viscosity and  $S$  is the shear stress.

### 2.4 Mass Transfer Model:

The Rayleigh Plesset model is implemented in the multiphase framework as an inter-phase mass transfer model in CFX code. For cavitating flow, the homogeneous multiphase model is typically used. In CFX, the mass transfer model is based on simplified Rayleigh Plesset equation which can be expressed as;

$$\dot{m} = \begin{cases} -F_v \frac{3r_{nuc}(1-\alpha)\rho_v}{R_B} \sqrt{\frac{2}{3} \frac{P_v - P}{\rho_l}} & \text{if } P < P_v \\ F_c \frac{3\alpha\rho_v}{R_B} \sqrt{\frac{2}{3} \frac{P - P_v}{\rho_l}} & \text{if } P > P_v \end{cases} \quad (8)$$

where,  $P_v$  is the liquid vapour pressure,  $r_{nuc}$  is the nucleation site volume fraction,  $R_B$  is the radius of a nucleation site,  $F$  is an empirical factor which may have different values for condensation and vaporization which is designed to account for the fact that they may occur at different rates. In CFX the above mentioned coefficients, by default are set as follow:  $r_{nuc} = 5 \times 10^{-4}$ ;  $R_B = 1.0 \times 10^{-6}$ ;  $F_v = 50$ ;  $F_c = 0.01$ . The validation of the Rayleigh Plesset cavitation model is used as presented by Bakir *et al.* (2004).

### 3. SIMULATION METHODOLOGY

The methodology is adopted in four steps. The first step is the preparation of geometry as per prototype machine dimension, second step is meshing the geometry of each parts, third step provides the boundary conditions as per data available from site selected and last step is the simulating the model and observe the results in the post processor.

#### 3.1 Modeling and Meshing

Francis turbine, the machine is divided in four components; spiral casing, stay and guide vanes, runner and draft tube. Fig. 1 shows the 3D model of the Francis turbine. The geometry model of each component for the flow domain has been prepared in Autodesk Inventor as shown in Fig. 1. The computational domain has been meshed using unstructured grid which consists of hexahedral, prism and tetrahedral elements.

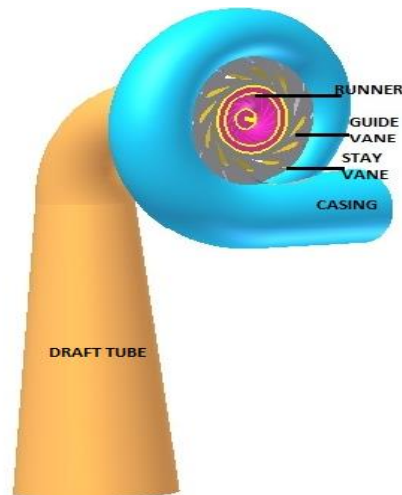


Fig. 1. 3-D model of Francis turbine.

Moreover, the pyramidal elements are set to connect hexahedral and tetrahedral elements. The meshing was generated using ANSYS ICEM CFD as shown in Fig.2. In order to minimize the influence of grid number on the computational results, a grid independency test has been carried out with three different meshes. Three different sets of mesh as coarse ( $\phi_1 = 6.9$  million), medium ( $\phi_2 = 15.67$  million) and fine ( $\phi_3 = 24.72$  million) are considered. The layer mesh was generated around the stay, guide vanes and blades for capturing the boundary layer. The quality mesh generated and the orthogonal quality ( $>0.4$ ), aspect ratio ( $<80$ ) and skewness ( $>0.8$ ) are found to be within the permissible limits.

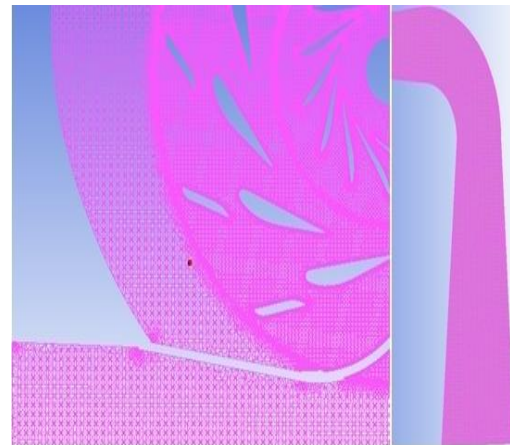


Fig. 2. Meshing on mid-plane of Francis turbine.

Based on the analysis, the different values of efficiency has been obtained as 84.28 %, 91.57 % and 92.12 % corresponding to grid elements values of 6.98, 15.67 and 24.72 million respectively and are shown in Fig. 3.

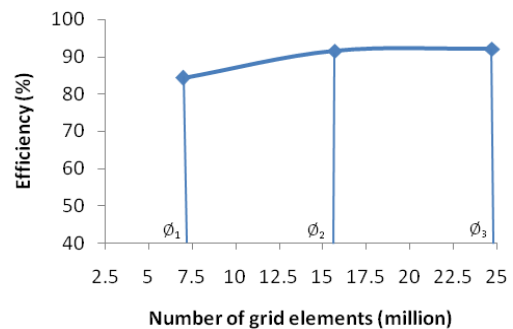


Fig. 3. Analysis of the number of grid elements.

Considering the efficiency correlation coefficient

which is defined as  $\xi = \frac{|\eta_m - \eta_s|}{\eta_m} * 100$  %, where;

$\eta_m$  and  $\eta_s$  are the values of predicted efficiency according to a large grid number and a small grid number, respectively (Liu *et al.*, 2013; Gohil and Saini, 2014). Its value is found to be less than 1% when the influence of the grid number was ignored. Finally, a total number of mesh elements of 15.6 million for the entire assembly was selected.

Gjosaeter, 2011 recommended the  $y^+$  value in the range of 20 to 200 for a Francis turbine runner. The  $y^+$  value is a non-dimensional distance from the wall to the first cell node.

It has been obtained in the logarithmic region range of 1.2 to 97. The details of mesh statics in each component is given in Table 2.

**Table 2 Details of mesh statics**

Component	Number of nodes	Number of elements
Casing	759423	4052846
Stay and Guide Vanes	1435454	5355339
Runner	1559018	5191533
Draft Tube	270246	1014592

### 3.2 Boundary Conditions

The geometry is set to make the inlet and outlet boundaries locations identical to the inlet and outlet locations considered during model testing in laboratory. Fig. 4 presents the locations of the boundary conditions and numerical computational domains of the turbine.

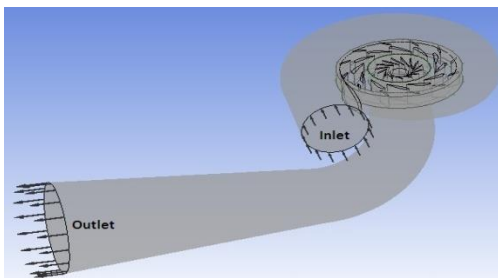


**Fig. 4. Computational domain of Francis turbine model.**

The four components have been used in simulation and complete CFD analysis system was accomplished at a plant sigma factor ( $\sigma_p$ ) of 0.17. Mass flow rate at inlet and pressure at outlet are widely accepted boundary conditions for the simulation of hydraulic turbo machines (Sudsuansee *et al.*, 2011; Zhang *et al.*, 2012; Zhang Rui *et al.*, 2013). All other components considered are a wall and the non-slipping flow condition. The casing, stay vane, guide vane and draft tube are stationary components while runner is considered under rotation. Rotational speed of the runner is considered as 750 rpm and components are attached with others by domain interface. The time step has been considered for 12 degree of revolution as 0.00266667 second. The SST turbulence model is used and a convergence criterion of maximum  $1E-4$  is considered with high resolution scheme. The SST model performance has been studied in a large number of cases. The SST-model was used as it has advantage of the strength of the  $k-\epsilon$  (free flow) and the  $k-\omega$  model (close to wall) (ANSYS Inc, 2010). For the cavitation case, the volume fraction of vapor and water were considered to be 0 and 1 respectively.

Under present study, extensive numerical simulation has been performed in operating range

from part load to over load. The three different flow rates conditions from part load to over load along with different values of guide vane angle are considered. In all cases steady state solution without cavitation was used as an initial condition for steady state calculation with cavitation and these results were used as an initial condition for unsteady analysis with cavitation. The range of input and output parameters is used as given in Table 3.

**Table 3 Values of Input and output parameters at boundary conditions**

	Inlet condition (mass flow rate, kg/s)	Outlet Condition (static pressure, Pa)
Part load	307	70937
Rated load	830	
Over load	1133	
Reference Pressure = 0 Pa		
Vapor Pressure = 3169 Pa (Temperature = 25°C)		

## 4. RESULT AND DISCUSSION

### 4.1 Hydraulic Efficiency Characteristic

The hydraulic efficiency is calculated using the relation which can be defined as;

$$\eta_h = \frac{T \times \omega}{(P_{ti} - P_{to}) \times \rho \times g} \quad (9)$$

where;  $P_{ti}$  and  $P_{to}$  are calculated of the total pressure [Pa] at inlet of casing and outlet of draft tube respectively,  $\omega$  is angular speed of runner [rad/s],  $T$  is the torque [Nm] produced by runner,  $\rho$  is the density of fluid [ $kg/m^3$ ] and  $g$  is the gravitational acceleration [ $m^2/s^2$ ] (Liu *et al.* 2011; Peng *et al.* 2010; Trivedi *et al.*, 2013).

The hydraulic efficiency has been computed by using Eq. (9) and compared with the model testing results (obtained from the manufacturer). In addition, three simulations are carried out to keep constant guide vane angle of  $20^\circ$  under different mass flow rates. It has been found that maximum efficiency is obtained at rated load condition (BEP).

Fig. 5 shows the comparison of the experimental and numerical hydraulic efficiency under cavitation and without cavitation conditions at three different operating points. It is seen that the efficiency of the turbine increases initially up to rated discharge and then decreases.

It has been found that the efficiency under cavitation condition was decreased by 1.05 %, 0.46% and 1.91 % for part load, rated load and overload operating conditions respectively. The predicted efficiency obtained by CFD analysis has a very good agreement with the efficiency obtained by model testing results. The error observed in the efficiency may be due to various assumptions made, modeling errors and discretization errors.

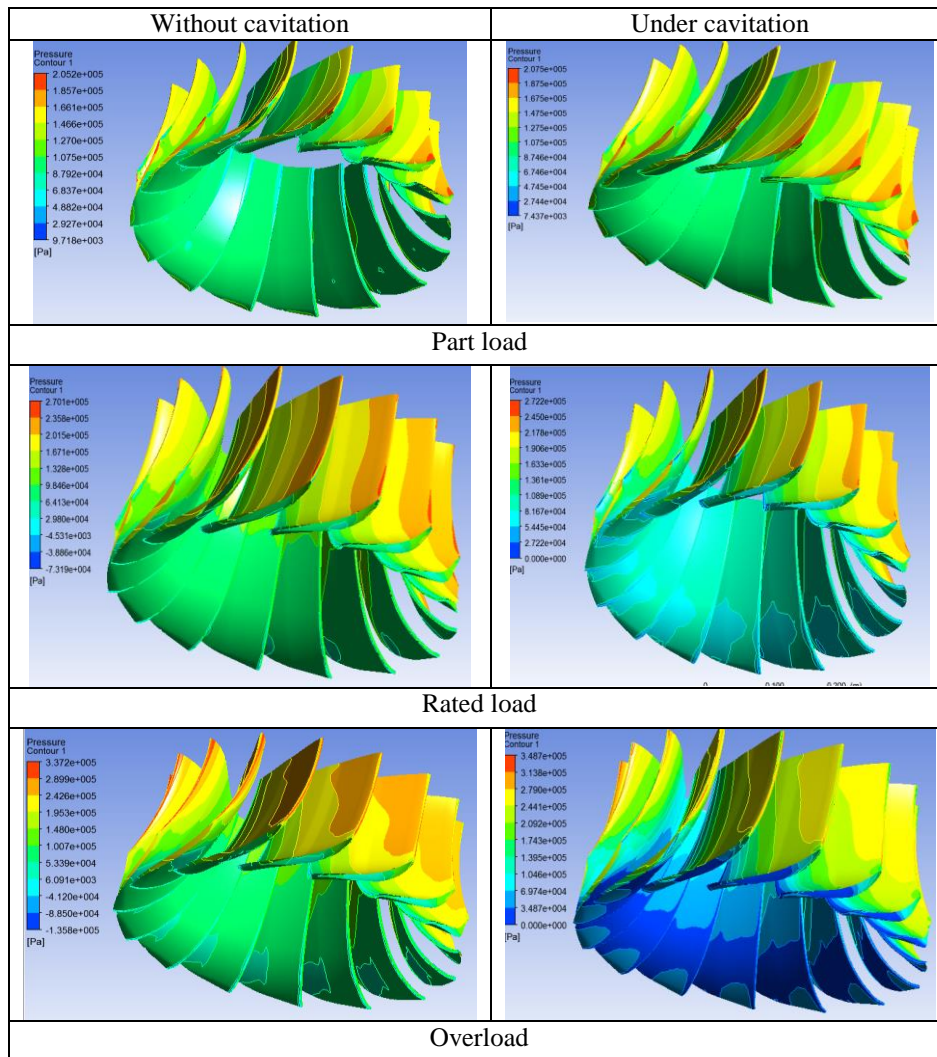


Fig. 6. Pressure distribution on runner under cavitation and without cavitation.

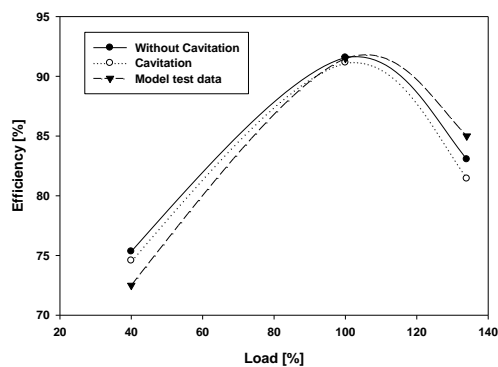


Fig. 5. Comparison of performance with model test data.

#### 4.2 Pressure Distribution Over Runner

The pressure distribution over runner for part load, rated load and overload conditions is obtained as shown in Fig. 6. It has been found that pressure decreases from inlet of casing to outlet of draft tube due to extraction of energy, and velocity increases from inlet to the outlet of the runner as per the

characteristics of reaction turbine.

A small variation of pressure distribution is observed over the surface of the blade under part load condition. However, more pressure difference has been found at overload condition in comparison to rated load condition.

It has been clearly seen that the low pressure value observed at suction side of trailing edge under overload condition. At leading edge, low pressure values are also observed under rated load condition.

#### 4.3 Pressure Fluctuation in Draft Tube

The behavior of pressure fluctuation or pulsation is an important feature to understand hydraulic turbine instability. The pressure points P1 and P2 are considered at 0.3D and 1D from the runner exit or the inlet of the draft tube, where D is the diameter of the runner according to IEC-60193 (1999) as shown in Fig 7. The pressure has been investigated in time domain at points P1 and P2 at part load, rated load and over load conditions under with and without cavitation conditions.

Fig. 8 and 9 shows the comparison of amplitude of pressure fluctuation at 0.3D and 1D respectively. It

is clearly seen that the pressure pulsation is higher at part load than at over load and rated load under with and without cavitation conditions. The flow is found as unstable and high pressure fluctuations were observed under part load condition. At rated load condition a very marginal difference in pressure pulsation between with and without cavitation conditions is observed.

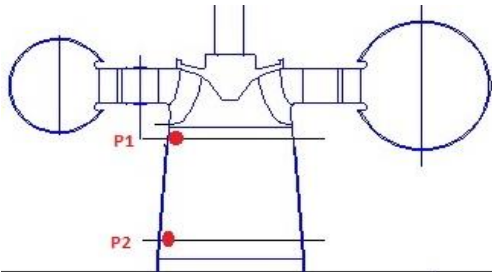


Fig. 7. Position of pressure measurement in the draft tube.

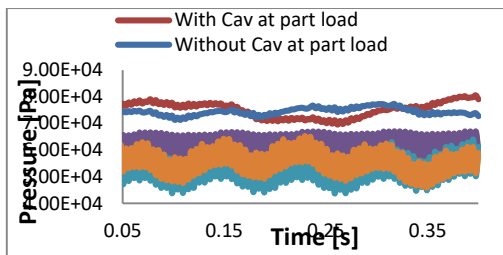


Fig. 8. Pressure pulsation in time domain at P1 (=0.3D).

Flow may be considered as stable and symmetrical under these conditions. Further at over load condition, the pressure pulsation difference is accountable but less than that of part load conditions at point, P<sub>1</sub>. This may be due to occurrence of large low pressure zone below the centre of runner hub which caused the water to cavitate. The pressure fluctuation enlarges with partial load of the Francis turbine was also reported in previous studies (Escaler *et al.*, 2006; Yulin *et al.*, 2011; Christopher, 1994). Similar, observation has been observed at point, P<sub>2</sub> as shown in Fig. 9. At point P<sub>2</sub>, it has been found that there is no random pressure fluctuation under rated load condition. The fluctuations in pressure is lesser than that of point, P<sub>1</sub> for all three cases.

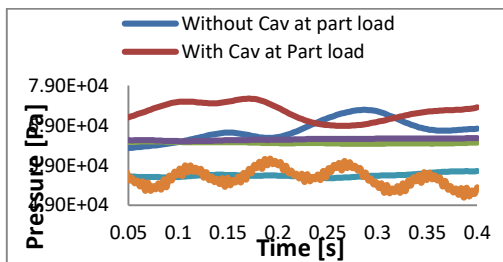


Fig. 9. Pressure pulsation in time domain at P2 (=1D).

#### 4.4 Vortex Rope

The vortex rope can be investigated in the

simulation by an iso-surface of vapor volume fraction, pressure and velocity.

In order to evaluate the 3D shape and the extent of cavity, iso-surface of vapor volume fraction ( $\alpha=0.5$ ) represents vortex ropes in the draft tube at plant sigma factor as obtained and is shown in Fig. 10 at part load, rated load and overload conditions. It shows a qualitative assessment of the cavity boundary.

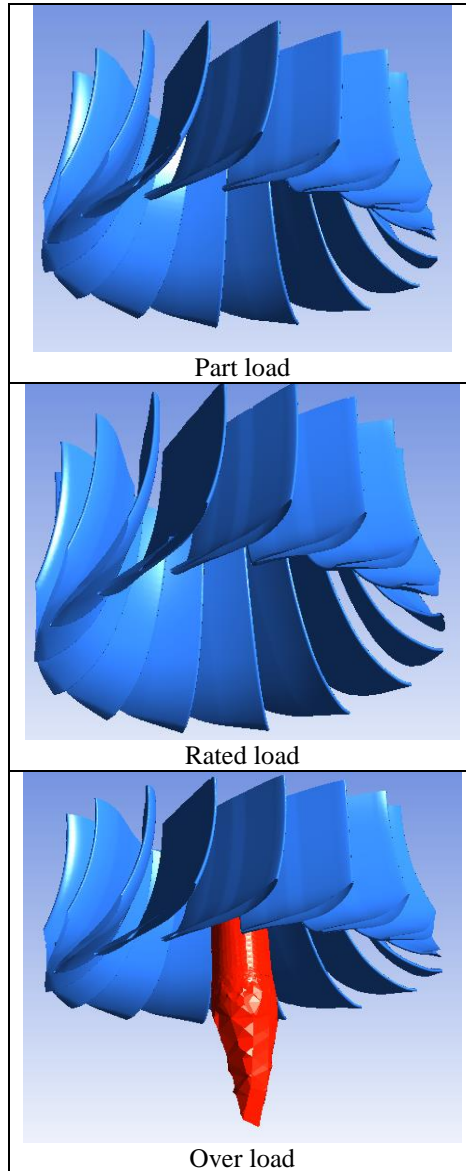
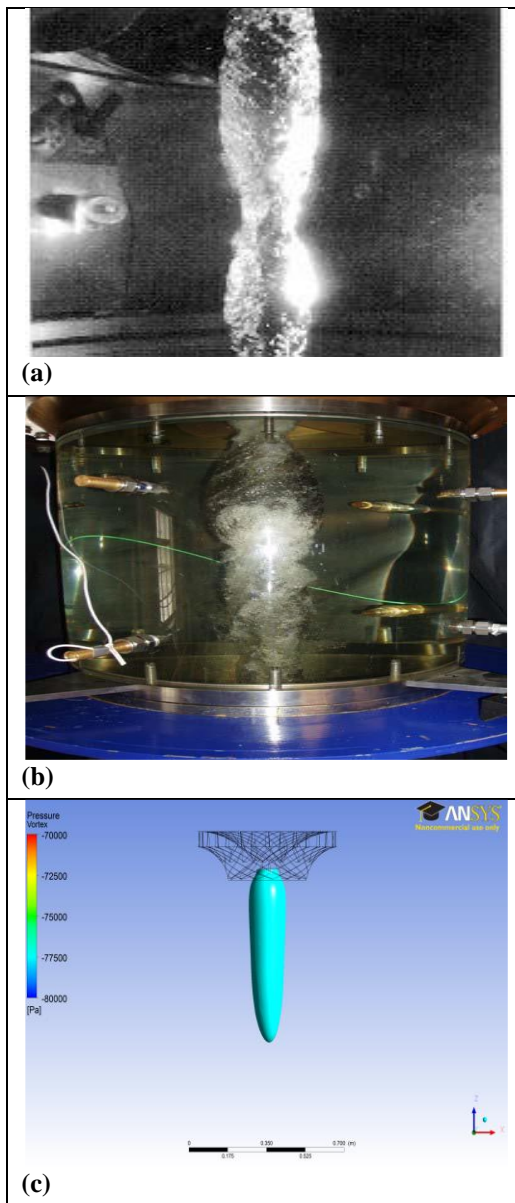


Fig. 10. Iso-surface of volume fraction in the draft tube.

It is clearly seen that the vortex rope phenomena is not observed at part load and rated load conditions. While at overload condition, straight vortex rope formation has been observed. A similar phenomenon of picture was observed in earlier studies as shown in Fig. 11. The numerical result has shown the shape of the vortex rope at over load which is very similar in nature with other studies (Avellan *et al.*, 2004; Einar, 2010; Simen, 2011).

#### 4.5 Volume Fraction of Water Vapour

The volume fraction of vapor is an important parameter for predicting cavitating flow in hydro turbines. The quantity is a fraction varies between 0 and 1, with a value of 1 indicating 100 % of vapor bubbles. The vapor bubbles are not seen under part load condition, but over load conditions these are observed relatively in more quantum at suction side of the runner. However, amount of vapor bubble are found to be marginal at leading edge of the blade at rated load condition is shown in Fig. 12. Fig. 13a illustrates the volume fraction of water vapor distribution over runner blade at over load condition. The quantum of vapor volume fraction has found to be increased from part load to over load condition.



**Fig. 11. Vortex rope in the draft tube at overload condition (a) picture of experiment [Avellan *et al.*, 2004], (b) picture of experiment [Einar, 2010], (c) simulation result of iso-surface of pressure [Simen, 2011].**

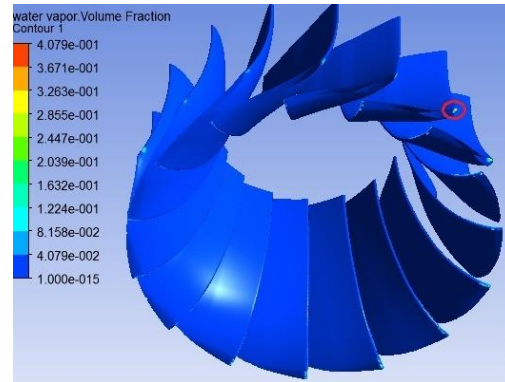


**Fig. 12. Vapor volume fraction on the runner at rated load.**

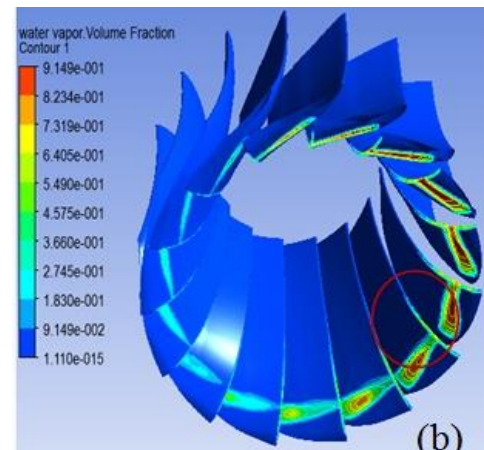
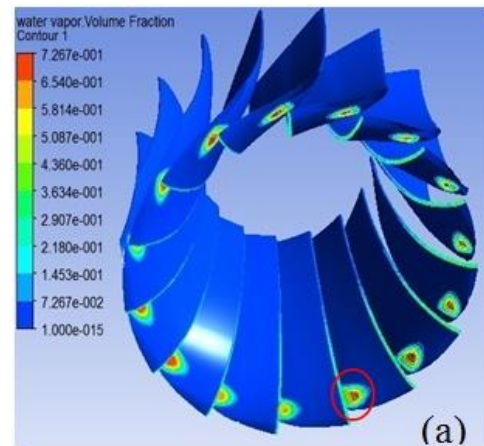


**Fig. 13. Vapor volume fraction on the runner.**

In order to observe the more effect of cavitation, one more simulation was run at less ( $\sigma = 0.13$ ) than plant sigma factor condition ( $\sigma < \sigma_p$ ).

It is clearly seen that the more vapor bubbles are formulated at suction side of runner blade (trailing edge) as illustrated as Fig. 13b. The results obtained are found to be on similar lines of results reported in earlier studies (Chrisopher, 1994). The area marked by circles in the Fig. 14 indicates the location of the cavitation damage. The numerical result has shown qualitative agreement for the location and extent of the cavitating zone.

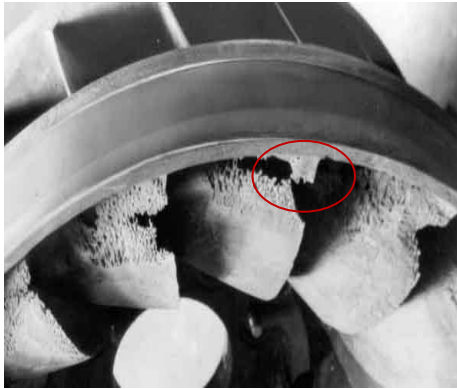


Fig. 14. Picture of actual cavitation damage runner [Christopher, 1994].

## 5. CONCLUSION

The CFD simulation results have prominently contributed to understanding the imprecisely complex, multiphase phenomenon of cavitation. In this paper, the simulation of cavitating turbulent flow through a whole passage of a prototype Francis turbine with SST turbulence model and cavitation model using Rayleigh-Plesset equation has been carried out. Based on the CFD analysis it has been found that the total computed efficiency loss is minimum at rated load operating point and maximum at overload condition. At over load condition, the more quantum of vapor bubbles formation was observed in the vicinity of trailing edge of runner blade. The pressure fluctuation has been found to be high at the inlet of draft tube under part load condition. A good agreement is found between the numerical results and the model test results forefficiency. The locations of cavitating zone observed during analysis are also validated with the results of previous studies.

## ACKNOWLEDGEMENT

Author (Pankaj Gohil) would like to express his gratitude to the QIP centre, IIT Roorkee for providing the financial assistance for the Ph. D. programme and his sponsored institute of Sarvajani College of Engineering and Technology, Surat. The technical support received from the Pentaflo Hydro Pvt. Ltd., New Delhi is gratefully acknowledged.

## REFERENCES

- Anslys, 13. (2010). *ANSYS CFX-Solver Theory Guide*. ANSYS Inc.
- Avellan F., P. Dupont, M. Farhat, B. Gindroz, P. Henry, M. Hussain, E. Parkinson and O. Santal (1990). Flow survey and blade pressure measurement in a Francis turbine model. *Proceeding of the XV IAHR symposium, Belgrade, Yugoslavia* 15(2), 1-14.
- Avellan F., P. Dupont, M. Farhat, B. Gindroz, P. Henry and M. Hussain (1993). Experimental flow study of the GAMM turbine model. In G. sottas and I. L. Ryhming (eds.), 3D-computation of incompressible internal flows. *NNFM* 3933-53.
- Avellan, F. (2004). Introduction to cavitation in hydraulic machinery. *The 6th International Conference on Hydraulic Machinery and Hydrodynamics Timisoara, Romania, October 21 – 22, 11-22*.
- Bakir F., R. Rey, A. G. Gerber, T. Belamri and B. Hutchinson (2004). Numerical and Experimental Investigations of the Cavitating Behaviour of an Inducer. *Int J Rotating Machinery* 10, 15-25.
- Bernad, S., S. Muntean, R. F. Susan-Resiga and I. Anton. (2004). Numerical Simulation of Two-Phase Cavitating Flow in Turbomachines. *International Conference on Hydraulic Machinery and Hydrodynamics* 4(22), 439–46.
- Bernad, S. and R. Susan-Resiga (2006). Numerical Analysis of the Cavitating Flows. *Proceedings of the Rom Academay Ser A* 7(1), 1–13.
- Christopher, E. B. (1994). *Hydrodynamics of Pumps*. Oxford University Press.
- Einar, K. (2010). *Measurement of Pressure Pulsations in Francis Turbines*. Ph. D. Thesis, NTNU Norway.
- Escaler, X., E. Egusquiza, M. Frahat, F. Avellan, M. Coussirat (2006). Detection of Cavitation in Hydraulic Turbines. *Mechanical Systems and Signal Processing* 20(4), 983–1007
- Franc, J. (2007). *The Rayleigh-Plesset equation: a simple and powerful tool to understand various aspects of cavitation: Fluid Dynamics of Cavitation and Cavitating Turbopumps*. Springer Wien, New York 1–41.
- Gohil Pankaj, P. and R. P. Saini (2014). CFD: Numerical Analysis and Performance Prediction in Francis Turbine. *Proceedings of 1st International Conference on Non Conventional Energy, Kalyani* 130-133.
- Gjosater. K. (2011) *Hydraulic design of Francis Turbine Exposed to Sediment Erosion*. Master thesis, NTNU, Waterpower laboratory, NTNU, Trondheim.
- Hou-lin, L., Dong-xi L., Y. WANG, X. WU and J. WANG. (2013). Application of modified k- $\omega$  model to predicting cavitating flow in centrifugal pump. *Water Science and Engineering* 6(3), 331-339.
- IEC 60193. (1999). standard. *Hydraulic turbines, storage pumps and pump-turbines-model acceptance tests*. International Electrotechnical commission, Geneva.
- Liu, S., and Q. Chen (2007). Unsteady cavitating turbulent flow simulation in Kaplan turbine 52(66).
- Peng, Y., X. Chen, Y. Cao and G. Hou (2010). Numerical Study of Cavitation on the Surface of

- the Guide Vane in Three Gorges Hydropower Unit. *Journal of Hydrodynamics, Ser. B* 22(5), 703–8.
- Simen R. B. (2011). *CFD analysis of the impeller and suction in a Francis turbine*. Master Thesis, NTNU Norway.
- Sudsuansee, T., U. Nontakaew and Y. Tiaple. (2011). Simulation of Leading Edge Cavitation on Bulb Turbine 33(1), 51–60.
- Trivedi, Chirag, M. J. Cervantes, B. K. Gandhi and Ole G. Dahlhaug. (2013). Experimental and Numerical Studies for a High Head Francis Turbine at Several Operating Points. *Journal of Fluids Engineering* 135(11), 111102-1-17.
- Water P. and D. C. Yearbook (2006). Wilmington Media Ltd.
- Wang, G., I. Senocak, W. Shyy, T. Ikohagi and S. Cao (2001). Dynamics of attached turbulent cavitating flows. *Progress in Aerospace Sciences* 37, 551-581.
- Wang, Y-C. and C. E. Brennen (1994). Shock wave development in the collapse of a cloud of bubbles. *ASME FED, Cavitation and Multiphase Flow* 194, 5-19.
- Yulin W., S. Liu, H. Dou and L. Zhang. (2011). Simulation of unsteady cavitating turbulent flow in a Francis turbine using the RANS method and the improved mixture model of two -phase flows. *Engineering with Computers* 27, 235-250.
- Zhang, L, J. T. Liu, Y. L. Wu and S. H. Liu (2012). Numerical Simulation of Cavitating Turbulent Flow through a Francis Turbine. *IOP Conference Series: Earth and Environmental Science* 15(6).
- Zhang, R. and Hong-xun Chen (2013). Numerical Analysis of Cavitation within Slanted Axial-Flow Pump. *Journal of Hydrodynamics, Ser. B*, 25(5), 663-72.